Research Journal of Applied Sciences, Engineering and Technology 3(1): 32-38, 2011
ISSN: 2040-7467

Received: September 03, 2010 Accepted: November 27, 2010 Published: January 20, 2011

Effective Stress-Porosity Relationship above and Within the Oil Window in the North Sea Basin

K.S. Okiongbo
Department of Geology and Physics, Niger Delta University, Wilberforce Island, Bayelsa State, Nigria

Abstract: This study investigates the effective stress - porosity relationship above and within the oil window in the Kimmeridge Clay Formation (KCF) in the North Sea Basin (UK) using effective stress and porosity determined from wireline logs and pore pressure data. Porosity was determined from an empirical porosity - sonic transit - time transform, calibrated using shale and mudstone core porosity measurements from Jurassic shales in the North Sea. Effective stress was determined from the total overburden stress and pore pressure. The total overburden stress was calculated by integration of the density log. The results show that porosity range between ~11-20% in the pre-generation zone but decreased to <5% within the oil window. Compaction coefficient (β) values above the oil window vary from ~0.08-0.09 M/Pa, but vary from ~0.05-0.06 M/Pa within the oil window implying that deeper burial and a high degree of chemical precipitation and cementation has created a stiff matrix giving rise to low β values. The effective stress-porosity relationship above and within the oil window reflects a possible decrease in effective stress occasioned by increase in porosity in the pre-generation zone.

Key words: Compaction coefficient, effective stress, mudstone, North Sea, pore pressure, porosity

INTRODUCTION

During petroleum generation at temperatures greater than 90ºC in a source rock, the solid phase kerogen is slowly converted to oil and gas and subsequently expelled. Cornford (1994) suggested that the conversion of kerogen to oil creates porosity, leaving a sufficient space for relatively good interconnectivity and thus increases permeability, and because of the overburden, fluid expulsion is enhanced, resulting in a considerably reduced porosity than the pre-generation zone. The compaction of a source rock in the pre-generation zone is due primarily to porosity reduction driven by mechanical and non-mechanical compaction but may be due to a composite of porosity reduction driven by mechanical and non-mechanical compaction and petroleum generation in the oil window.

Mechanical compaction is thus an inevitable consequence of burial and basin evolution. As such, several empirical porosity/depth trends have been published in an attempt to explore the relationship between compaction of shale sediments and depth of burial in different sedimentary basins (Sclater and Christie, 1980; Hansen, 1996). Depth, however, is primarily a position co-ordinate that specifies present-day location. Depth is therefore a poor measure of the processes that have acted upon a sedimentary section through time (Schmoker and Gautier, 1989). Theoretical models and observational data indicate that equilibrium porosities do not typically persist through geologic time. Rather, diagenetic processes (and the resulting compaction of basin sediments) tend to continue as long as porosity exists. As a result, depth of burial offers an incomplete basis for porosity evaluation and modelling. Conventional models of shale compaction therefore relate porosity to effective stress using the empirical relationship between void ratio and effective stress established in soil mechanics (Burland, 1990; Yang and Aplin, 2004).

In this study, we explore the effect of petroleum generation by evaluating the variation in porosity and effective stress in the Kimmeridge Clay Formation (KCF) above and within the oil window. The model we employed (the compaction law) is based on a simple relation between porosity and effective stress that assumes no change in rock matrix properties (expressed through the compaction coefficient β) with time.

Study area: The northern North Sea is the area North of 55ºN (the Mid North Sea high) to about 62ºN, and includes all basins within the area both in the UK and Norwegian sectors of the North Sea (Fig. 1). Its geological evolution has been extensively discussed in various papers (Nielsen *et al*., 1986; Thorne and Watts, 1989). The North Sea is a Paleozoic to Holocene multistage rift basin within the north western European cratonic block. It is superimposed on the Caledonian Orogenic trend. The tectonic framework of the northern North Sea consists of a north-trending Viking Graben,

Fig. 1: Map of the study area showing well locations

which intersects in the South, the South easterly-orientated Central Graben and the westerly Witch Ground Graben.

The lithologies are composed of sands and shales in the Triassic-Jurassic section of the basin and locally organic matter (e.g., Kimmeridge Clay) is present. In the Cretaceous, the lithologies are dominantly carbonates and shales. They are mainly shales, silts and sands in the Tertiary with an interruption in the Paleocene when Volcanism occurred. This corresponds to the widespread deposits of volcanic tuffs all over the graben (Hancock, 1990).

MATERIALS AND METHODS

Since the main objective is to explore the effect of petroleum generation and expulsion on the porosity and effective stress in the KCF in the North Sea Basin, UK, we have used the resistivity log to elucidate wells in which the KCF is immature and those in which the KCF is within the main phase of hydrocarbon generation and expulsion. We have used the resistivity log (LLD) because the resistivity log is maturity dependent (Stocks and Lawrence, 1990), and as such, resistivities are expected to increase in source rocks and most significantly in the presence of free hydrocarbons generated by thermal maturity. We observe that the electrical resistivities in the West of Shetland wells (205/20-1, 204/27A-1, 35/11-4, and 204/23-1) range between ~ 2-5 ohms consistent with the resistivities of immature source rock reported elsewhere in the North Sea by Cornford (1994). Temperature data in these wells range between 44-90ºC indicating that the KCF in these wells is immature.

In contrast, selected wells in the Halten Terrace and Mid North Sea High (34/8-6, 30/9-14, 6407/1-2, and 25/2-6) show significant increases in resistivity. We observe a relatively rapid depth-related change from low to high resistivity values from 3875-4075 m. These reductions in the electrical conductivity of the sediment are totally consistent with many of the shale pores being oil wet at least around peak oil generation depths (3000-4000 m) (Cornford, 1994). Our Hydrogen Index (HI) and temperature data (HI decreased from ~400 to <50 mgHC/gTOC, while temperature increased from <90 to ~157ºC) is also consistent with this. We believe that the KCF in these wells is mature and is believed to be in the main phase of hydrocarbon generation and expulsion. Therefore wireline log (e.g., sonic, density, resistivity, gamma ray logs) and pore pressure data were thus selected from these eight wells for compaction coefficient (β) estimation.

Additionally, twenty-two core samples from 15 wells taken from the central and northern parts of the North Sea and the Norwegian Margin were selected for porosity measurement. The samples were taken from a depth range of ~ 1.5–5.0 km, and a bottomhole temperature data range from 44-157ºC. Porosity was determined from the shale core samples using mercury porosimetry technique based on the approach of Katsube and Williamson (1998), and were calibrated against transit time values from the sonic log recorded at depths in the wells where the cores were recovered to obtain a sonic transit time-to-porosity transform. The transform is as follows:

$$\Phi = 1 - \left(\frac{66.8}{\Delta t}\right)^{1/3.31} \quad (1)$$

Effective stress is expressed as:

$$\sigma_v^1 = \frac{1}{\beta}\left[\ln\left(\frac{\Phi_0}{\Phi}\right)\right] \quad (2)$$

where,

Φ_o is a reference porosity and β (compaction coefficient) is an empirical constant.

Effective stress on a rock matrix can also be determined as:

$$\sigma_v^1 = S_v - P_f$$

where, S_v (expressed as $\rho_g gh$) is the lithostatic or overburden stress and P_f is the pore fluid pressure.

Total overburden stress (S_v) was calculated by integration of the density log, but since the logging run rarely starts from the sediment-water interface, we have estimated the magnitude of the overburden stress in the unlogged section (i.e., sediment-water interface to the

depth at which the density log starts its run) by using the method introduced by Yang and Aplin (2004) for the North Sea. The equation is as follows:

$$\sigma_v = 0.01799*Z + 9.95*10^{-7}*Z^2 \quad (3)$$

where, Z is true vertical depth from the sea floor in metres and σ_v is vertical stress from the sea floor (MPa). Also, stresses were evaluated at 1m interval in the logged section using the bulk density values derived from the density log. The value of σ_v obtained from Eq. (3) was then added to the values of stresses determined at approximately 1m intervals. This was done cumulatively. Thus, the total overburden stress (Sv) at any depth was obtained using the relationship

$$Sv = 0.01799*Z + 9.95*10^{-7}*Z^2 + \rho_b g\Delta Z \quad (4)$$

where,
Sv = total overburden stress (MPa)
ρ_b = bulk density (g/cm^3)
g = acceleration due to gravity (m/s^2)
ΔZ = 1.0 m

The pore pressure data was mainly from adjacent sand intervals to the KCF (from the gamma ray log). This data was used to constrain the pore pressure within the KCF using the following relation:

Pore pressure (shale)
= Pore pressure (sand) - $\rho_w g\Delta Z$ (5)

where,
ρ_w = density of water
ΔZ = depth difference between KCF interval and sand in which pore pressure was measured

Having constrained the pore pressure in the KCF, we evaluated the vertical effective stress (σ_v') using Eq. (2). We also evaluated $\ln(\Phi_0/\Phi)$, where Φ_0 is an assumed initial porosity (80%), and Φ are porosities determined at those intervals in which the pore pressure data was taken. Having evaluated values for σ_v' and $\ln(\Phi_0/\Phi)$, we used Eq. (6) to evaluate the compaction coefficient (β) at each depth interval.

$$\beta = 1/\sigma_v' * \ln(\Phi_o/\Phi) \quad (6)$$

The compaction coefficients determined for the KCF above and within the oil window are shown in Table 1. We averaged the β values in wells 205/20-1, 204/27A-1 and 35/11-4 in an attempt to evolve a regional effective stress-porosity plot above the oil window. Also, β values for wells, 204/23-1, 34/8-6, 30/9-14, 6407/1-2 and 25/2-6 were averaged to evolve a regional effective stress-porosity plot within the oil window. Having found averaged values of β above and within the oil window, Eq. (2) was used to calculate the effective stresses both above and within the oil window using the sonic log derived porosities from Eq. (1).

Table 1: Compaction coefficients determined for the KCF

	Well no.	Depth (m)	Compaction coeff. (β)(M/Pa)
KCF above oil window	205/20-1	1940-1944	0.0938
	204/27A-1	2030-2048	0.0830
	35/11-4	1901-1916	0.0906
	204/23-1	3785-3788	0.0460
KCF within oil window	34/8-6	3501-3542	0.0646
	30/9-14	2964-2994	0.0624
	6407/1-2	3528-3814	0.0510
	25/2-6	3083-3239	0.0545

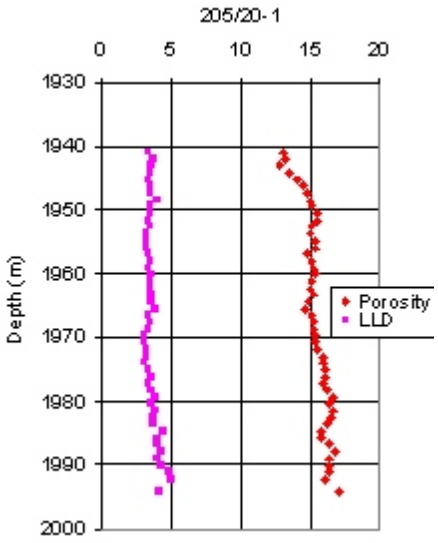

Fig. 2: Crossplot of porosity and resistivity against depth (205/20-1)

RESULTS AND DISCUSSION

The variation of porosity with depth both above and within the oil window in the KCF is shown in Fig. 2-9. Above the oil window, we observe that porosities vary from ~ 11-20% (Fig. 2-4). Since the porosity - transit time transform was calibrated using porosities determined from cores selected from organic rich intervals against transit time values recorded at depths in the wells where the cores were recovered, we believe that these porosities are a reflection of the true porosity of the KCF above the oil window. However, we did not observe a decrease in porosity as depth increases (Fig. 2) typical of a normally compacted porosity profile. We conjectured therefore that inhibited efficient dewatering and consolidation of the low permeable shales in the KCF may have contributed to the porosity-depth profiles observed in Fig. 2 and 3 which we believe is anomalous and perhaps indicates generation of high pore fluid pressure. In contrast, porosities

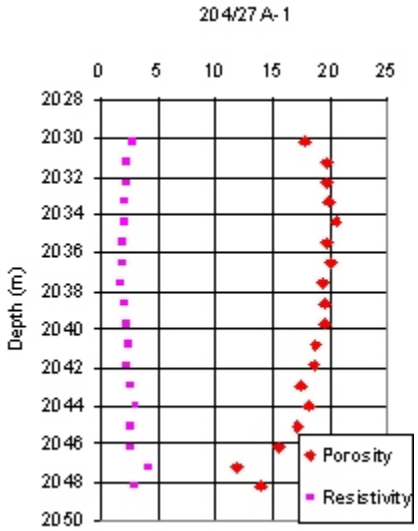

Fig. 3: Crossplot of porosity and resistivity against depth (204/27A-1)

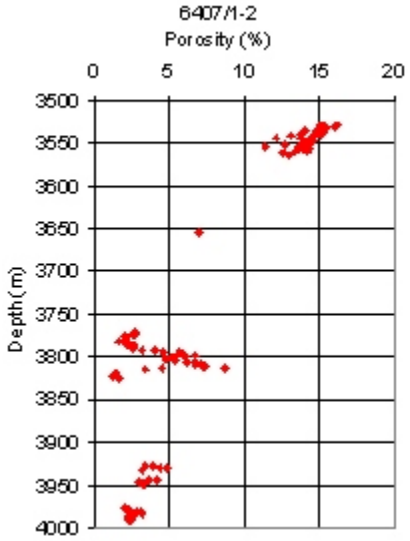

Fig. 4: Porosity as a function of depth (6507/2-3)

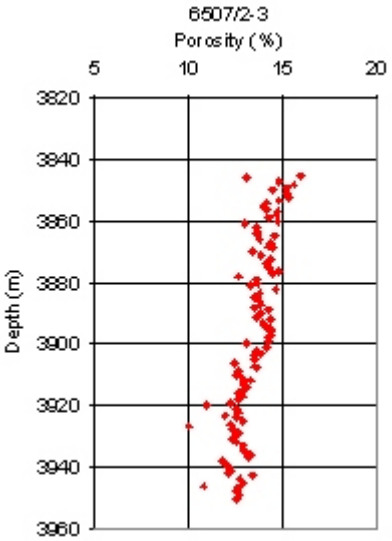

Fig. 5: Porosity as a function of depth (6407/1-2)

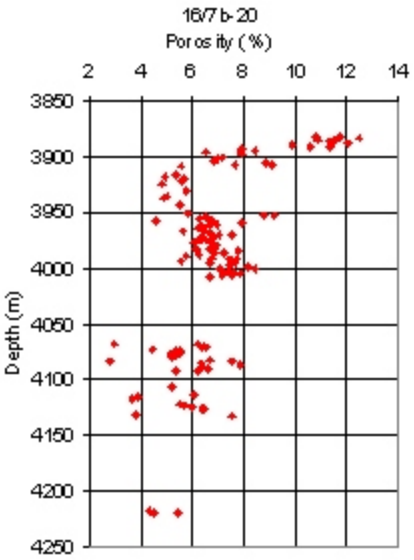

Fig. 6: Porosity as a function of depth (16/7b-20)

decreased from 11-20% to <5% except well 6507/2-3 within the oil window (Fig. 4-9). We are tempted to believe that the porosity difference between the zone of pre-generation and within the oil window is largely a function of the sediment permeability. Macleod *et al.* (1996) suggested that the conversion of kerogen to oil creates porosity, leaving a sufficient space for relatively good inter-connectivity and thus increases permeability, and because of the overburden, fluid expulsion is enhanced, resulting in a considerably reduced porosity values than the pre-generation zone. It suggests therefore, that the KCF above the oil window may be less permeable compared to the oil window.

The compaction coefficients (β) determined for the KCF both above and within the oil window are shown in Table 1. Above the oil window, β values vary from ~0.08-0.09 M/Pa. Within the oil window, β varies from ~0.05-0.06 M/Pa. A plot of void ratio (e) against $\ln(\sigma'_v/100)$ (Aplin *et al.*, 1995; Fig. 8) shows that β increases from 0.05 at e<1.0 to 0.45 at e>4.0. The implication of this plot is that less consolidated sediments are characterised with greater β values than highly consolidated sediments. In the same publication, Aplin *et al.* (1995) reported β values of 0.20 to 0.65 for a

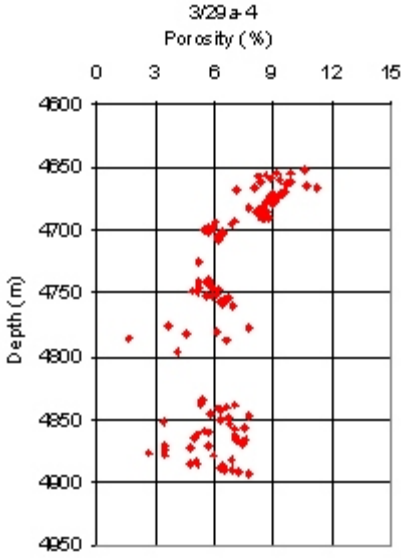

Fig. 7: Porosity as a function of depth (3/29a-4

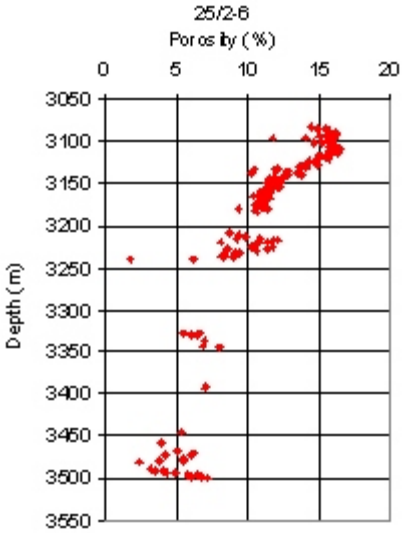

Fig. 8: Porosity as a function of depth (25/2-6)

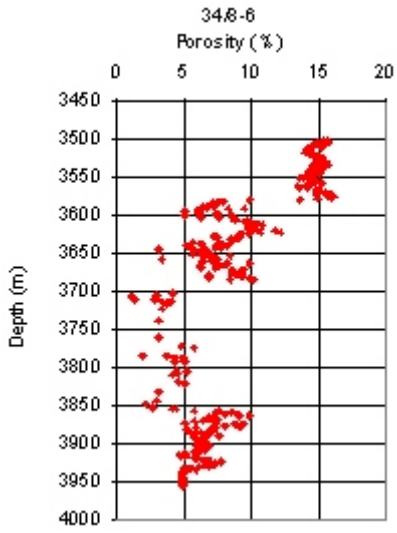

Fig. 9: Porosity as a function of depth (34/8-6

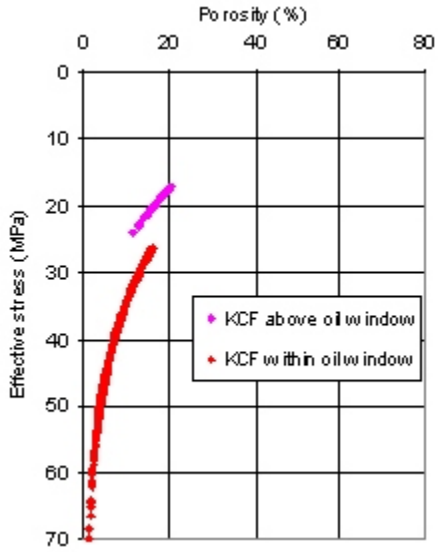

Fig. 10: Effective stress as a function of porosity above and within the oil window

set of North Sea samples not significantly affected by diagenesis at the depth range of 690-2444 m, thereby extending the range of Burland's (1990) data (0.08-0.45). Nygard *et al.* (2004) reported β-values of 0.211 and 0.060 for a less compacted Kimmeridge Westbury clay and a fully cemented Kimmeridge Bay clay. The literature evidence above shows that β-values for sediments ranges between $0.05<\beta\geq0.60$. In general, weak, uncompacted sediments have β-values close to unity. With continuing compaction, sediments become stronger and their β-value decreases.

We compared the β values determined in this study with these published values. We observed that the range (0.05-0.09) is in good agreement with the value of 0.06 reported by Nygard *et al.* (2004) for a fully cemented Kimmeridge Bay clay. We infer therefore that deeper burial and a high degree of chemical precipitation and cementation has created a stiffer matrix giving rise to the low β values obtained in this study in the KCF at the depth range of ~2.0-4.7 km. The discrepancy between β-values obtained in this study with those reported by Aplin *et al.* (1995) is presumably due to the exclusion of chemically compacted sediments in the dataset of the later.

The variation of β observed in Table 1 shows that the use of a single value of compaction coefficient for

different parts of the KCF may be inappropriate and re-emphasizes the fact that non-mechanical processes may also be important. Furthermore, the mechanical compaction model used in determining the compaction coefficients may be inappropriate as these samples may have been influenced by varying degree of diagenesis.

In this study, we relate effective stress to porosity. The model we employed (the compaction law) is based on a simple relation between porosity and effective stress that assumes no change in rock matrix properties (expressed through the compaction coefficient β) with time. Therefore, time-dependent relaxation of the rock matrix due to under compaction occasioned by variations in fluid pressure through lateral transfer (Yardley and Swarbrick, 2000) or the cracking of oil to gas during burial of sediments is not described by this model. Figure 10 shows effective stress porosity relationship above and within the oil window. A common interpretation of the effective stress-porosity relationship above and within the oil window as observed in Fig. 10 is that the loss of porosity is faster in the pre-generation zone than within the oil window. One may in addition suggest that the effective stress-porosity trend within the oil window might be a reflection perhaps of the fact that cementation and deeper burial has created a relatively stiffer matrix for the KCF sediments within the oil window making it more difficult to compact at high effective stresses. But above, we observed that porosity ranged between ~ 1-20% in the pre-generation zone but decreased to <5% in the oil window. We conjectured therefore that due to the anomalous nature of the porosity-depth plots above the oil window, the oil window may be relatively more permeable perhaps due to the transformation of solid kerogen to petroleum. We are convinced therefore that the interpretation that porosity loss is faster in the pre-generation zone as may be inferred from the effective stress-porosity relationship above and within the oil window in Fig. 10 is not a plausible explanation.

Rather, the effective stress-porosity trend in the pre-generation zone reflects a possible decrease in effective stress. Yang and Aplin (2004) developed relationships between compression coefficients and clay content from natural, fine-grained clastic sediments. Yang and Aplin's (2004) model is based on well data from the North Sea and as well as data derived from the studies of Skempton, (1970) and Burland (1990). The relationships are as follows:

Skempton-Burland data:

$$e_{100} = 0.659 + 0.592Clay + 2.424Clay^2 \quad (7)$$

$$\beta = 0.0686 + 0.0937Clay + 0.0937Clay^2 \quad (8)$$

North Sea data:

$$e100 = 0.3024 + 1.6867Clay + 1.9505Clay^2 \quad (9)$$

$$\beta = 0.0407 + 0.2479Clay + 0.3684Clay^2 \quad (10)$$

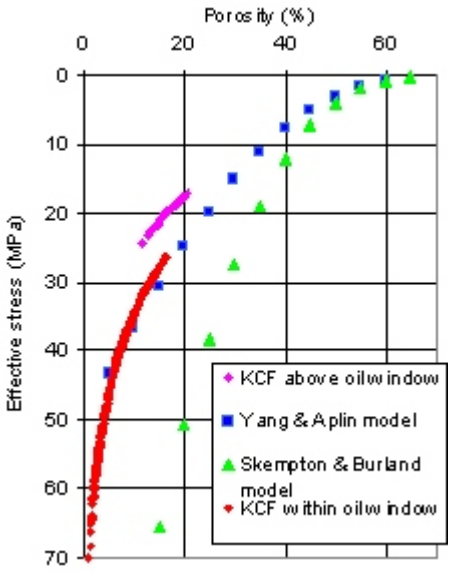

Fig. 11: Comparison between effective stress-porosity trends derived from Skempton-Burland and Yang and Aplin data published by Yang and Aplin (2004) and data from this study

The compression coefficients e_{100} (void ratio at 0.1MPa effective stress) and β were determined by using an assumed clay content of 65% for purposes of comparison with results of this study. This is because it is assumed that the KCF has a clay content of about 65%. The estimated compression coefficients were then substituted in the basic compaction equation given below:

$$\sigma' = 100.\exp(e_{100} - e/\beta) \quad (11)$$

Figure 11 compares the compression curves from Skempton-Burland and North Sea dataset published by Yang and Aplin, (2004), and that presented in this study. Although the clay content is assumed to be the same (~65%) in all the datasets, a remarkable difference exists in terms of their organic carbon content. Skempton (1970) and Burland (1990) datasets are low TOC samples (TOC <1 wt %), the North Sea dataset used by Yang and Aplin, (2004) have TOC ranging between 1-5%, whilst the current dataset have TOC ranging between 5-10%. Besides, Yang and Aplin's (2004) dataset exclude chemically compacted sediments. Above the oil window, the Figure indicates similarity between the trend of Yang and Aplin (2004) and that from this study on extrapolation to low effective stresses (<5 MPa). Significant variation only occurs at effective stresses >5 MPa which is attributed to reduced effective stresses occasioned by increased porosity. Within the oil window, the Figure shows a perfect match between the compaction trend derived from the Yang and Aplin's (2004) data and that derived from data presented in this study. It is difficult to

make firm conclusions between the dataset of Yang and Aplin (2004) and that used in this study based on the effective stress-porosity trends, especially within the oil window as observed in Fig. 11. But perhaps it indicates that no fundamental differences exist in the nature of the compaction process in deep-burial settings between the two datasets.

CONCLUSION

The variation of porosity above and within the oil window plotted as a function of depth and effective stress show a wide variability in porosity. Porosity ranged between ~11-20% in the pre-generation zone but decreased to <5% in the oil window. The compaction profiles in the pre-generation zone are indeed atypical of normal shale compaction curves at these depths and we attribute it to inhibited efficient dewatering and consolidation of the low permeable shales and perhaps indicates generation of high pore fluid pressure. Compaction coefficients (β) values above the oil window vary from ~0.08-0.09 M/Pa, but vary from ~0.05-0.06 M/Pa. We infer that deeper burial and a high degree of chemical precipitation and cementation has created a stiff matrix giving rise to the low β values in this study in the KCF at the depth range of ~2.0-4.7 Km. The variation of β suggests that the use of a single value of β for different parts of the KCF is inappropriate. The effective stress - porosity trend above the oil window reflects a possible decrease in effective stress occasioned by increase in porosity. The mechanical compaction model used in determining the compaction coefficients may be inappropriate as the samples may have been influenced varying degrees of diagenesis.

ACKNOWLEDGMENT

I wish to thank the Bayelsa State Government, Nigeria for sponsoring my post-graduate research. I wish to also thank A.C.Aplin and Steve Larter for the pastoral care during my PhD.

REFERENCES

Aplin, A.C., Y. Yang and S. Hansen, 1995. Assessment of Beta, the compression coefficient of mudstones and its relationship with detailed lithology. Mar. Petrol. Geol., 12: 955-963.

Burland, J.B., 1990. On the compressibility and shear strength of natural clays. Geotechnique, 40: 329-378.

Cornford, C., 1994. Mandal-Ekofisk (!) Petroleum System in the Central Graben of the North Sea. In: Magoon, L.B. and W.G. Dow (Eds.), The Petroleum System - from Source to Trap. AAPG Memoir, 60: 537-571.

Hancock, J.M., 1990. The Cretaceous. In: Glennie, K.W. (Ed.), Introduction to the Petroleum Geology of the North Sea. Blackwell Scientific Publications, pp: 255-272.

Hansen, S., 1996. A compaction trend for Cretaceous and Tertiary shales on the Norwegian Shelf based on sonic transit times. Petrol. Geosci., 12: 159-166.

Katsube, T.J. and M.A. Williamson, 1998. Shale Petrophysical Characteristics: Permeability History of Subsiding Shales. In: Schieber, J., W. Zimmerle and P. Sethi (Eds.), Shales and Mudstones, 11: 69-91.

Macleod, G., M. Bigge and S.R. Larter, 1996. A preliminary assessment of the influence of volume changes in sedimentary organic matter. Geopop Progress Report of the University of Newcastle, Fourth Six Monthly Report (Unpublished).

Nielsen, O.B., S.S. Sorensen, J. Thiede and O. Skarbo, 1986. Cenozoic differential subsidence of the North Sea. AAPG, 70: 276-298.

Nygard, R., R. Gautam and K. Hoeg, 2004. Compaction behaviour of argillaceous sediments as a function of diagenesis. Mar. Petrol. Geol., 21: 349-362.

Schmoker, J.W. and D.L. Gautier, 1989. Compaction of Basin sediments: Modelling based on time-temperature history. J. Geophys. Res., 94(B6): 7379-7386.

Sclater, J.G. and P.A.F. Christie, 1980. Continental stretching: An explanation of the Post-Mid-Cretaceous subsidence of the central North Sea Basin. J. Geophys. Res., 85: 3711-3739.

Skempton, A.W., 1970. The consolidation of clays by gravitational compaction. Q. J. Geol. Soc. London, 125: 373-411.

Stocks, A.F. and S.R. Lawrence, 1990. Identification of Source Rocks from Wireline Logs. In: Hurst, A., M.A. Lovell and A.C. Morton (Eds.), Geological Applications of Wireline Logs. Geological Society Special Publication, 48: 241-252.

Thorne, J.A. and A.B. Watts, 1989. Quantitative analysis of North Sea Subsidence. AAPG, 73: 88-116.

Yardley, G.S. and R.E. Swarbrick, 2000. Lateral transfer, a source of additional pressure? Mar. Petrol. Geol., 17: 523-537.

Yang, Y. and A.C. Aplin, 2004. Definition and practical application of mudstone porosity-effective stress relationships. Petrol. Geosci., 10: 153-162.